We are IntechOpen, the world's leading publisher of Open Access books Built by scientists, for scientists

6,900
Open access books available

185,000
International authors and editors

200M
Downloads

Our authors are among the

154
Countries delivered to

TOP 1%
most cited scientists

12.2%
Contributors from top 500 universities



WEB OF SCIENCE™

Selection of our books indexed in the Book Citation Index in Web of Science™ Core Collection (BKCI)

Interested in publishing with us?
Contact book.department@intechopen.com

Numbers displayed above are based on latest data collected.
For more information visit www.intechopen.com



Chapter 5

OFDM Systems for Optical Communication with Intensity Modulation and Direct Detection

Jian Dang, Liang Wu and Zaichen Zhang

Additional information is available at the end of the chapter

http://dx.doi.org/10.5772/intechopen.68199

Abstract

Intensity modulation and direct detection (IM/DD) is a cost-effective optical communication strategy which finds wide applications in fiber communication, free-space optical communication, and indoor visible light communication. In IM/DD, orthogonal frequency division multiplexing (OFDM), originally employed in radio frequency communication, is considered as a strong candidate solution to combat with channel distortions. In this research, we investigate various potential OFDM forms that are suitable for IM/DD channel. We will elaborate the design principles of different OFDM transmitters and investigate different types of receivers including the proposed iterative receiver. In addition, we will analyze the spectral efficiency and decoding complexities of different OFDM systems to give a whole picture of their performance. Finally, simulation results are given to assess the detection performance of different receivers.

Keywords: OFDM, optical communication, IM/DD, modulation, detection

1. Introduction

Optical communication is an important part of modern communication techniques due to the excessive bandwidth of the light spectrum. Theoretically, optical communication has much higher system throughput than its radio frequency (RF) communication counterpart. Therefore, it finds many applications and facilitates our lives. Some typical optical communication scenarios include optical fiber communication, free-space optical communication, and visible light communication. In those communication scenarios, intensity modulation and direct detection (IM/DD) is a cost-effective communication scheme compared to coherent ones. In IM/DD, the intensity, or power, of the light beam from a laser or a light-emitting diode (LED) is modulated by the information bits and no phase information is needed. Due to this nature, no local oscillator is required for IM/DD communication, which greatly eases the cost of the hardware.

INTECH
open science | open minds

© 2017 The Author(s). Licensee InTech. This chapter is distributed under the terms of the Creative Commons Attribution License (http://creativecommons.org/licenses/by/3.0), which permits unrestricted use, distribution, and reproduction in any medium, provided the original work is properly cited. CC BY

In IM/DD channel, there are still some non-ideal factors that may deteriorate the quality of communication. One key factor is the multipath effect. This effect is caused by several mechanisms. First, in wireless communications, the light could be reflected at multiple locations and by many times by the surroundings before arriving at the receiver side. Second, the modulation bandwidth of LED is limited, typically below 100 MHz. When the bandwidth of signal exceeds the modulation bandwidth of LED, multipath effect occurs. Third, in fiber communication, light components of different wavelength propagate through different paths, which also cause multipath effect. Therefore, effective means of mitigating the multipath effect are necessary in IM/DD optical communications.

In RF communication, orthogonal frequency division multiplexing (OFDM) is a powerful multi-carrier modulation scheme to combat the multipath effect. Compared to the single-carrier modulation schemes, OFDM avoids the usage of a complicated high-order time-domain equalizer. Instead, it employs frequency domain equalizer that only has a single tap. This greatly simplifies the equalization task and can perfectly resolves the multipath effects without any residual errors at high signal-to-noise ratio (SNR) region. Thus, introducing OFDM to IM/DD optical communication is a natural choice. However, different from RF communication, IM/DD requires that the transmitted signal must be real and positive, which imposes strict constraint on the modulation scheme and the original OFDM transceiver must be modified carefully to satisfy the new scenario. In addition, different applications may have diverse emphasis such as spectral efficiency, power efficiency, detection capability, as well as computational complexity.

Within such perspectives, the purpose of this chapter was to analyze the potential forms of OFDM that are suitable for IM/DD transmission as well as various receiver designs in optical communication. We first study the concepts and basic modulation schemes of OFDM systems in IM/DD optical communication. They can be generally classified into three categories: direct-current-biased optical OFDM (DCO-OFDM), non-DC-biased optical OFDM, and hybrid optical OFDM. We will elaborate the system models and explain the validity of some fancy designs in those systems through analysis. Second, we investigate the preliminary receivers of those OFDM systems. Besides, we will propose a new receiver that is capable of improving the detection performance based on the inherent signal structures of the specific transmitted signal. Third, the spectral efficiencies and computational complexities of different systems and receivers are analyzed and compared. Finally, the bit error rate (BER) performance of different systems is compared through computer simulations to give the reader a whole picture of different candidate OFDM systems in IM/DD optical communication.

2. OFDM principles

This section gives a brief introduction on the principles of OFDM in radio frequency communication which serves as a basis for further reading. The baseband diagram of OFDM is shown in **Figure 1**. At the transmitter side, coded information bits are first mapped to symbols through digital modulation such as pulse amplitude modulation (PAM), quadrature amplitude modulation (QAM), and phase shift keying (PSK). Typically, complex-valued QAM modulation is used

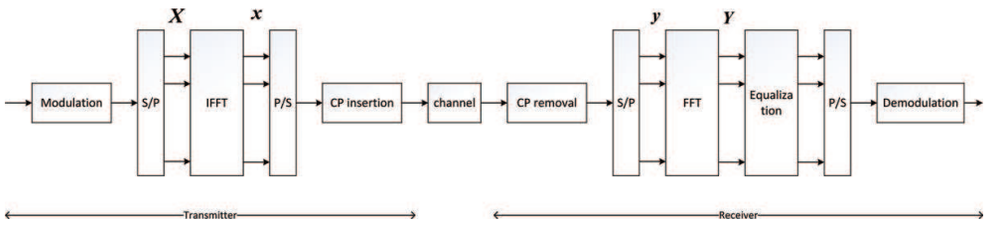


Figure 1. The "IFFT" module at the receiver side should be "FFT" module.

in OFDM. Then, the modulated symbols are divided into multiple groups and each group consists of N-modulated symbols, defined as $\boldsymbol{X} = [X(0), X(1), \ldots, X(N-1)]^T$, where the group index is omitted here for simplicity. In OFDM, each modulated symbol $X(k)$ is loaded on a *subcarrier* with center frequency $\frac{2\pi}{N}k$ and there are N subcarriers in total. All the symbols are transmitted on their subcarriers simultaneously. Mathematically, this is equivalent to transform the vector $\boldsymbol{X}$ by an N-point inverse fast Fourier transform (IFFT) module, resulting in a new vector $\boldsymbol{x} = [x(0), x(1), \ldots, x(N-1)]^T$, that is,

$$x(n) = \frac{1}{\sqrt{N}} \sum_{k=0}^{N-1} X(k) e^{j\frac{2\pi}{N}kn}. \tag{1}$$

In OFDM, $\boldsymbol{X}$ is generally considered as *frequency* domain signal and $\boldsymbol{x}$ is viewed as *time*-domain signal. In addition, $\boldsymbol{x}$ is typically called an *OFDM symbol*, which is different with the *modulated symbol* aforementioned. Finally, $\boldsymbol{x}$ is appended at its head with a cyclic prefix (CP), which is just the copy of the last few samples of $\boldsymbol{x}$. In general, the length of CP is no smaller than the length of transmission channel to avoid inter-symbol interference (ISI) between adjacent OFDM symbols.

Assuming the impulse response of the multipath channel is denoted by $\boldsymbol{h} = [h(0), h(1), \ldots, h(L-1)]^T$; then, the received signal at the receiver after channel transmission is given by

$$r(n) = h(n) * x_c(n) + z(n), \tag{2}$$

where $x_c(n)$ is the CP-appended version of the time-domain transmitted signal, $z(n)$ is the additive white Gaussian noise (AWGN) with zero mean, and * denotes linear convolution. The receiver first removes the CP parts of received signal, which results in a new vector $\boldsymbol{y}$ of length N, which can be rewritten as

$$y(n) = h(n) \otimes x(n) + z(n), \tag{3}$$

where $\otimes$ denotes cyclic convolution. We can see that due to the insertion and removal of CP, the linear convolution is now transformed to a cyclic one, which would be beneficial for equalization, as will be shown in the following text.

From signal processing theory, cyclic convolution in time domain is equivalent to product in frequency domain. Based on this fact, by defining $Y(k)$, $H(k)$, and $Z(k)$ as the N-point fast Fourier transform of $y(n)$, $h(n)$, and $z(n)$, respectively, one has

$$Y(k) = H(k)X(k) + Z(k), k = 0, 1, \ldots, N-1. \tag{4}$$

As we can see, each frequency-domain symbol $X(k)$ is transmitted as if in a *flat* channel of response $H(k)$ and different symbols transmit in different subchannels (subcarriers) without interfering with each other. This greatly simplifies the equalization task. For example, both zero forcing (ZF) and minimum mean square error (MMSE) equalization can be performed to recover $X(k)$ which only involves single-tap equalizer per subcarrier:

$$\widehat{X}(k) = \begin{cases} \dfrac{Y(k)}{H(k)}, & ZF \\ \dfrac{H^*(k)Y(k)}{|H(k)|^2 + {\sigma_n}^2}, & MMSE \end{cases} \tag{5}$$

where ${\sigma_n}^2$ is the variance of noise. The processing in Eqs. (4) and (5) can be realized by performing FFT and per-subcarrier equalization, as shown in **Figure 1**.

3. Optical OFDM systems for IM/DD channel

3.1. Preliminaries

In IM/DD channel, there is a key difference with RF channel: the transmitted signal must be real and positive. This results from the fact that the intensity of light must be a real and positive quantity. Therefore, the structure for OFDM shown in **Figure 1** cannot be directly used in IM/DD optical channel. Necessary changes must be made instead. A common approach is to generate a real time-domain signal first. This can be realized by imposing *Hermitian symmetry* on the frequency domain signal $\boldsymbol{X}$, which is defined as follows:

$$X(N-k) = X^*(k), k = 1, \ldots, N-1, X(0) = X(N/2) = 0. \tag{6}$$

It can be easily shown that the IFFT of $\boldsymbol{X}$ having property Eq. (6) is a pure *real*-valued signal $\boldsymbol{x}$. Based on this real signal, one can further generate a positive signal to drive the optical source by various means. Those resultant new OFDM systems are typically referred to as *optical OFDM* systems.

3.2. DC-biased optical OFDM

The most straightforward approach to generate a positive signal from a real signal is to impose a proper DC bias. In optical communication, the DC bias is typically chosen such that the mean value of the positive signal just lies on the center point of the linear range of the optical source. This system is called direct current-biased optical OFDM, or DCO-OFDM, whose transmitter is shown in **Figure 2**.

The clipping module shown in **Figure 2** is necessary. Since $x(n)$ is Gaussian distributed, it is possible that $x(n)$ plus a DC bias is still out of the linear range of the optical source. For example, if an LED accepts driving current within the range of $[a, b]$, where $0 \leq a < b$, then the

http://dx.doi.org/10.5772/intechopen.68199

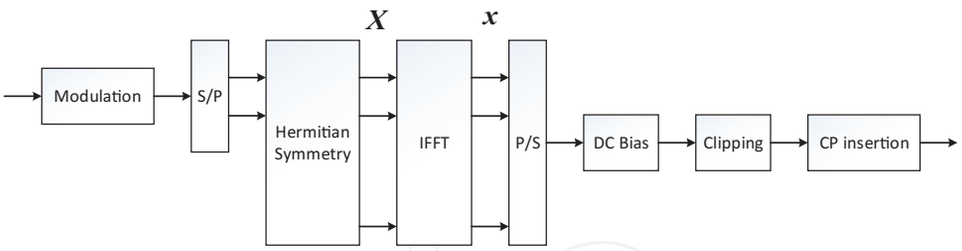


Figure 2. Diagram of DCO-OFDM transmitter.

clipping is needed to confine $x(n)$ plus a DC bias into this range. Otherwise, the LED could not be illumined due to under-driving or even be damaged due to over-driving.

3.3. Non-DC-biased optical OFDM

Besides DCO-OFDM, there are many forms of optical OFDM systems that are not relying on DC bias. The most famous ones are introduced in this subsection.

3.3.1. ACO-OFDM

Asymmetrically clipped optical OFDM (ACO-OFDM) is the most famous non-DC-biased optical OFDM system and has been extensively studied in literature [1]. The basic idea of ACO-OFDM is to generate an asymmetrically structured time-domain signal such that direct clipping at zero (without adding DC bias) is allowed without any information loss. To do so, the frequency-domain input symbol $\boldsymbol{X}$ has a special structure besides satisfying Hermitian symmetry. Specifically, the *odd* components of $\boldsymbol{X}$ contain useful information $\boldsymbol{U}$ but the *even* components of $\boldsymbol{X}$ are set to zeros. This is shown in **Figure 3**.

After IFFT, the time-domain signal $\boldsymbol{x}$ has an asymmetrical structure:

$$x(n) = -x\left(n + \frac{N}{2}\right), n = 0, 1, \ldots, N/2. \tag{7}$$

As shown in **Figure 4**, signal $\boldsymbol{x}$ can be directly clipped at zero without adding any DC bias, yet the information is kept after clipping thanks to the asymmetrical structure.

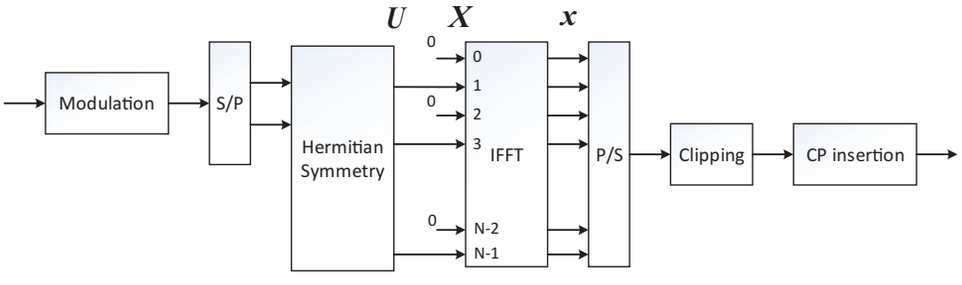


Figure 3. Diagram of ACO-OFDM transmitter.

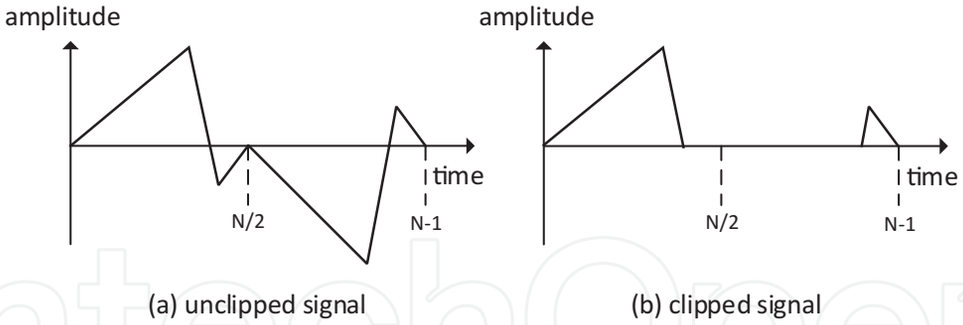


Figure 4. Asymmetrical structure before and after clipping at zero in ACO-OFDM.

3.3.2. PAM-DMT

Pulse amplitude modulation-discrete multi-tone (PAM-DMT) is another non-DC-biased optical OFDM system [2]. It is similar to ACO-OFDM, in that direct clipping is used. However, the difference is that in PAM-DMT, only the imaginary part of subcarrier input $\boldsymbol{X}$ carries useful information $\boldsymbol{U}$ while the real part is set to zero, as shown in **Figure 5**. Note that PAM modulation should be used in PAM-DMT rather than QAM in DCO-OFDM and ACO-OFDM.

It can be easily shown that the resultant time-domain signal $\boldsymbol{x}$ also has an asymmetric structure but is slightly different with that of ACO-OFDM, which is shown in Eq. (8) and **Figure 6**:

$$x(n) = -x(N-n), n = 1, 2, \ldots, \frac{N}{2}, x(0) = x\left(\frac{N}{2}\right) = 0. \tag{8}$$

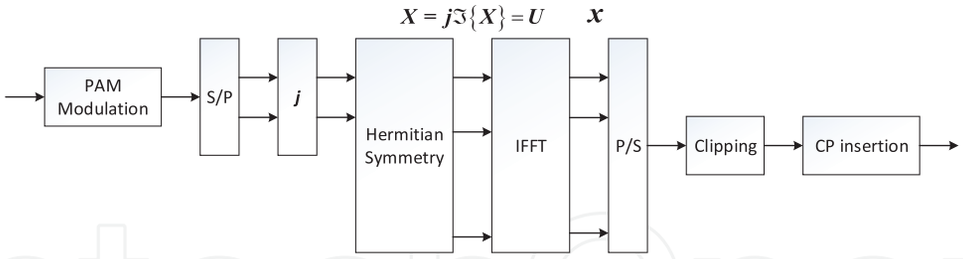


Figure 5. Diagram of PAM-DMT transmitter.

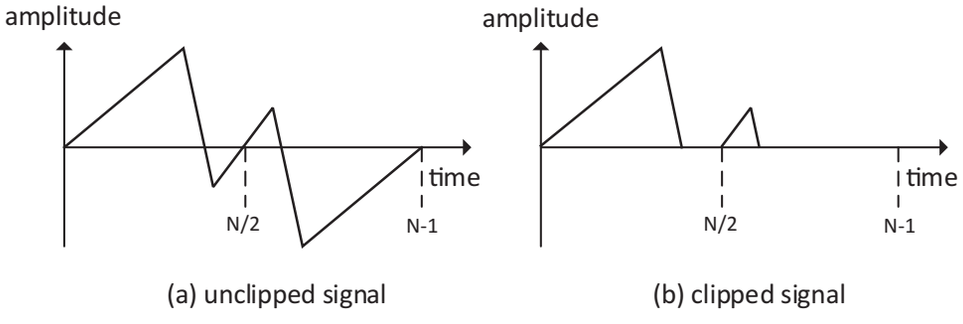


Figure 6. Asymmetrical structure before and after clipping at zero in PAM-DMT.

3.3.3. Flip-OFDM

Both ACO-OFDM and PAM-DMT rely on specially designed signal structures on the frequency- and time-domain signals. In contrast, flip-OFDM employs a simpler way such that a general frequency-domain signal $\boldsymbol{X}$ without any fancy structure is accepted [3]. Instead, the real time-domain signal $\boldsymbol{x}$, without any symmetry, is split into two parts: the first part only contains the samples of positive ones in $\boldsymbol{x}$, the negative ones are set to zeros; the second part only contains the samples of negative ones, but with flipped signs, and leaves the positive ones as zeros. This is shown in **Figure 7**.

Mathematically, the first and second parts of the flipped signal are given by

$$x_1(n) = \frac{x(n) + |x(n)|}{2}, x_2(n) = \frac{-x(n) + |x(n)|}{2}, n = 0, 1, \ldots, N-1. \tag{9}$$

After flip processing, the two signal parts are appended with CP, respectively, and are transmitted on channel consecutively. In some literature, flip-OFDM is also referred to as unipolar OFDM (U-OFDM).

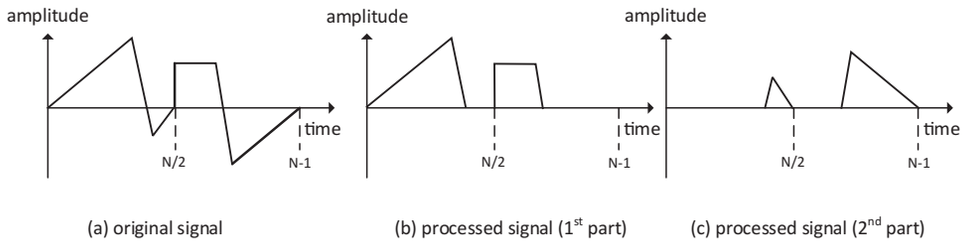


Figure 7. Signal structure before and after flipping processing in flip-OFDM.

3.4. Duality of non-DC-biased optical OFDM systems

This section gives a brief introduction on the duality of the non-DC-biased optical OFDM systems. Based on this duality, many receiver design methods could be easily extended from one system to other systems.

For ACO-OFDM, the transmitted signal is given by

$$x_c = (x + |x|)/2, \tag{10}$$

and $\boldsymbol{x}$ can be written as $\boldsymbol{x} = [\boldsymbol{x}_1; -\boldsymbol{x}_1]^T$, where $\boldsymbol{x}_1$ is the first half of $\boldsymbol{x}$. Therefore, the first and second halves of $\boldsymbol{x}_c$ can be written as

$$x_{c,1}(n) = \frac{x_1(n) + |x_1(n)|}{2}, x_{c,2}(n) = \frac{-x_1(n) + |x_1(n)|}{2}, \tag{11}$$

which is exactly the same as the model in Eq. (9) except that the size is changed from N to $N/2$.

For PAM-DMT, the transmitted signal is also given by Eq. (10). However, the unclipped signal $\boldsymbol{x}$ is slightly different, that is, $\boldsymbol{x} = [\boldsymbol{x}_1; \boldsymbol{x}_2]^T$, where $\boldsymbol{x}_2 = -\boldsymbol{J}\boldsymbol{x}_1$ with $\boldsymbol{J}$ being a matrix whose

anti-diagonal elements are 1s and other elements are all 0s. Now, the first and second halves of the transmitted signal are given by

$$x_{c,1} = \frac{x_1 + |x_1|}{2}, x_{c,2} = \frac{-Jx_1 + J|x_1|}{2}. \tag{12}$$

However, $\boldsymbol{JJ = I}$; therefore, by defining $\boldsymbol{x}_{c,3} = \boldsymbol{J}\boldsymbol{x}_{c,2}$, we have

$$x_{c,1} = \frac{x_1 + |x_1|}{2}, x_{c,3} = \frac{-x_1 + |x_1|}{2}. \tag{13}$$

Now, Eq. (13) is exactly the same as Eqs. (9) and (11).

Therefore, we can see that ACO-OFDM, PAM-DMT, and flip-OFDM essentially share the same signal structure and there is a duality between them. Based on this fact, the receivers designed for one system can be readily extended to other systems with simple substitution of variables.

3.5. Hybrid systems

Beside the basic forms of DC and non-DC-biased optical OFDM systems, there also exist some hybrid ones where multiple basic systems are superimposed in a specially designed fashion. In general, hybrid systems can be further classified into three categories.

3.5.1. Hybrid optical OFDM based on DCO-OFDM and a non-DC-biased one

A representative for this kind of system is ADO-OFDM, which combines DCO-OFDM and ACO-OFDM in a special way [4]. Specifically, in ACO-OFDM, the useful data are only loaded on the odd subcarriers, as illustrated in **Figure 3**, the even subcarriers are forced to be zero. After clipping in time domain, the clipping noise only falls onto even subcarriers and the odd subcarriers are not affected by the clipping noise. At the receiver side, the data could be recovered by using only the odd subcarriers. With the recovered data, one can further perfectly reconstruct the clipping noise on even subcarriers. Therefore, in ACO-OFDM, the even subcarriers can be exploited to load more data, which is the basic idea of ADO-OFDM.

In ADO-OFDM, the odd subcarriers are performed exactly the same as the ACO-OFDM. For the even subcarriers, a modified DCO-OFDM signal is generated, in which only the even subcarriers are used. Then, the signals generated from ACO-OFDM and DCO-OFDM are added together to obtain the ADO-OFDM signal. At the receiver side, ACO-OFDM signal, which is on odd subcarriers, are first detected. Then, the clipping noise on even subcarriers is estimated and subtracted. After that, the even subcarriers contain only DCO-OFDM signal, which is finally decoded.

3.5.2. Hybrid optical OFDM based on two different non-DC-biased ones

HACO-OFDM, or hybrid ACO-OFDM, combines ACO-OFDM and PAM-DMT in one system [5]. The basic idea is similar to that of ADO-OFDM, that is, the odd subcarriers are used for ACO-OFDM transmission while the even subcarriers are used for PAM-DMT transmission.

At the receiver side, interference cancellation is used for even subcarriers before decoding PAM-DMT signal. An alternative form for HACO-OFDM is also proposed [6].

3.5.3. Hybrid optical OFDM based on a same non-DC-biased one

Another form of hybrid optical OFDM is to superimpose multiple blocks of signals from a same non-DC-biased OFDM system. For example, enhanced unipolar OFDM (eU-OFDM) involves multiple blocks of signals from flip-OFDM [7]. **Figure 8** shows its time-domain structure with three layers [8], where the symbols $x_{i,j}^{+}$ and $x_{i,j}^{-}$ denote, respectively, the positive and flipped negative parts of the original j-th bipolar signal $x_{i,j}$ from layer-i. Each layer is just a repetition of flip-OFDM time-domain signal. We can see that for the first layer, four normal flip-OFDM symbols are used. For the second layer, two normal flip-OFDM symbols are repeated two times. For the third layer, one normal flip-OFDM symbol is repeated four times. Then, all the time symbols from three layers are added for transmission.

The receiver detection is very simple. The first layer is firstly decoded using normal subtraction. The second and third layers do not interfere in this procedure due to perfect self-cancellation. After the first layer is decoded, its impact is subtracted from the received signal. Then, the second layer is decoded subsequently. Then, the second layer signal is subtracted from the received signal and the third layer is decoded finally.

Besides eU-OFDM, the overlapping of ACO-OFDM or PAM-DMT is also proposed in literatures [9–11]. They all share similar idea with eU-OFDM and the receiver is based on layer-by-layer decoding.

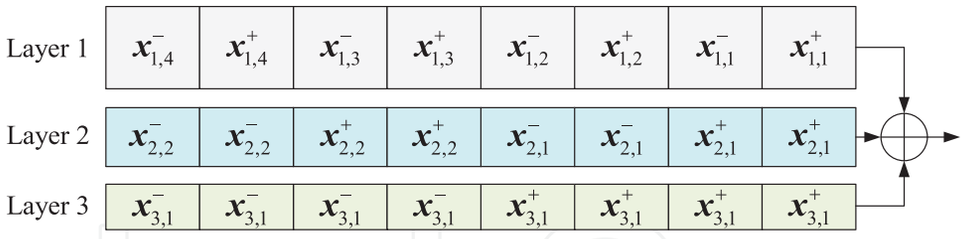


Figure 8. Illustration of a three-layer eU-OFDM time-domain signal components.

4. Receiver design for optical OFDM systems

In this section, we investigate the receiver design for optical OFDM systems. For DCO-OFDM, the receiver is straightforward. For non-DC-biased optical OFDM systems, there exist multiple candidate receivers which will be detailed later. For hybrid systems, since they are constructed mainly based on non-DC-biased ones, the receivers designed for non-DC-biased systems are also applicable for hybrid systems. Moreover, as the duality between non-DC-biased systems, in this chapter we focus on ACO-OFDM. We review the basic receiver design, diversity combining receiver design, and propose an iterative receiver design. All the formulations are based on an AWGN channel model but the results can be readily extended to multipath channels.

4.1. Basic receiver

The basic receiver for ACO-OFDM is very simple. The received signal after CP removal is given by

$$y(n) = x_c(n) + z(n). \tag{14}$$

In frequency domain, one has

$$Y(k) = X_c(k) + Z(k). \tag{15}$$

As proved by Ref. [1], the odd subcarriers of $X_c(k)$ is related to $X(k)$ by

$$X_c(k) = \frac{1}{2}X(k), \text{ for odd } k. \tag{16}$$

Therefore, the data $\boldsymbol{U}$, which is only on odd subcarriers of $\boldsymbol{X}$, can be recovered from $Y(k)$ by

$$\widehat{U}(k) = \begin{cases} 2Y(2k+1), & ZF \\ \dfrac{2Y(2k+1)}{1+{\sigma_n}^2}, & MMSE \end{cases} \qquad k = 0, 1, \ldots, \frac{N}{2} - 1 \tag{17}$$

The receiver diagram is shown in **Figure 9**.

4.2. Diversity combining receiver

The basic receiver only utilizes the odd subcarriers for signal detection. The even subcarriers, bearing pure clipping noise, are simply discarded. Therefore, half of the received power is wasted. However, the clipping noise has a special inherent signal structure that is dependent on the unclipped signal. This inherent signal structure could be exploited for better detection performance. This is the basic idea of diversity combining receiver and the iterative receiver.

To unveil the relationship between the clipping noise and the unclipped signal, we rewrite the clipped signal as

$$x_c(n) = \frac{1}{2}[x(n) + |x(n)|], \forall n. \tag{18}$$

Based on Eqs. (16) and (18), one can see that the clipping noise falls only onto the even subcarriers and has a special form as

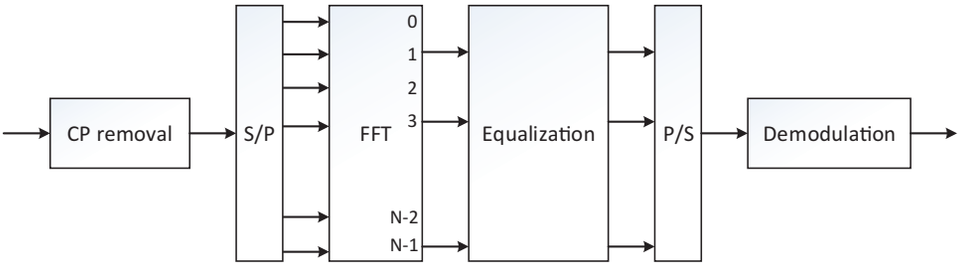


Figure 9. Diagram of the basic receiver for ACO-OFDM.

http://dx.doi.org/10.5772/intechopen.68199

$$X_c(k) = \frac{1}{2} FFT\{|x(n)|\}, \text{ for even } k, \tag{19}$$

which says that the clipping noise on the even subcarriers is just the FFT of $|x(n)|$. Thus, we can generate two signals based on $Y(k)$: the first one is $\boldsymbol{Y}_0 = [0 \quad Y(1) \quad 0 \quad Y(3) \ldots 0 \quad Y(N-1) \quad]^T$, and the second one is $\boldsymbol{Y}_e = [Y(0) \quad 0 \quad Y(2) \quad 0 \ldots Y(N-2) \quad 0]^T$. Denoting their time-domain signal by $\boldsymbol{y}_0$ and $\boldsymbol{y}_e$, respectively, we have

$$y_0 = \frac{1}{2} x + z_0, \tag{20}$$

$$y_e = \frac{1}{2} |x| + z_e. \tag{21}$$

Eq. (21) is obtained from Eqs. (16) and (19). A new signal $y_c(n)$ is generated based on Eqs. (20) and (21):

$$y_c(n) = \begin{cases} y_e(n), \text{ if } & y_0(n) \geq 0, \\ -y_e(n), \text{ if } & y_0(n) < 0. \end{cases} \tag{22}$$

Now, we get two branches of signals that are related to $x(n)$. Thus, diversity combining technique could be used to enhance the detection performance. The diversity combining is performed by

$$r(n) = a y_0(n) + (1-a) y_c(n), \forall n. \tag{23}$$

The combining coefficient a is usually a bit larger than 0.5 since $y_c(n)$ is not as accurate as $y_0(n)$ [12]. Based on $r(n)$, the data could be estimated just as in the basic receiver. The whole procedure of diversity combining receiver is shown in **Figure 10**.

A pairwise-ML receiver based on noise cancellation has been proposed in [13]. It has been proved that this receiver is in fact a special case of diversity combining receiver with a = 0.5 [14].

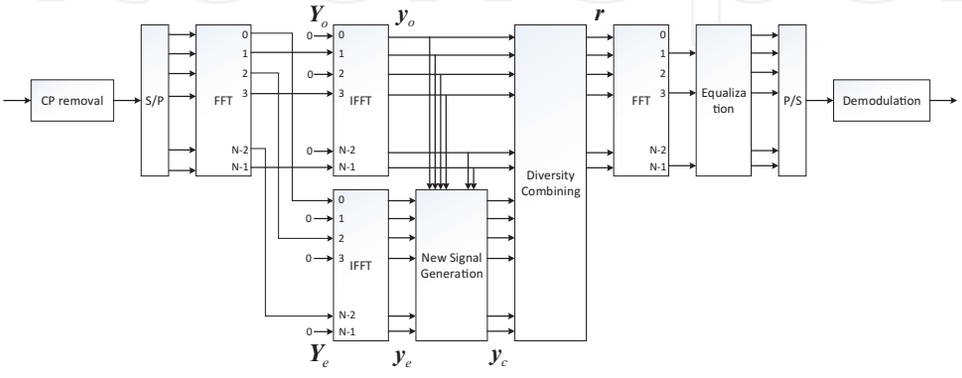


Figure 10. Diagram of diversity combining receiver for ACO-OFDM.

4.3. Proposed iterative receiver

Although the diversity combining receiver exploits the signal on even subcarriers, it is not performed in an optimal way, resulting in possible performance loss compared to optimal joint detection. Here, we propose an iterative receiver that has a better way to exploit the signal on even subcarriers [14]. The basic idea is to re-estimate the modulated data in a complete mathematical model at each iteration. At the very first iteration, the basic receiver is used for initialization. The details are given as follows.

Define an N by $N/2$ matrix $\boldsymbol{P}_0$ whose odd rows form an identity matrix and even rows are all zeros. Similarly, define another N by $N/2$ matrix $\boldsymbol{P}_e$ whose even rows form an identity matrix and odd rows are all zeros. Then, we have

$$\boldsymbol{X} = \boldsymbol{P}_0\boldsymbol{U},\ \boldsymbol{U} = \boldsymbol{P}_0{}^T\boldsymbol{X} = \boldsymbol{P}_0{}^T\boldsymbol{P}_0\boldsymbol{U}. \tag{24}$$

In addition, based on Eqs. (16) and (19), we have

$$\boldsymbol{P}_0{}^T\boldsymbol{X}_c = \frac{1}{2}\boldsymbol{U}, \tag{25}$$

$$\boldsymbol{P}_e{}^T\boldsymbol{X}_c = \frac{1}{2}\boldsymbol{W}|\boldsymbol{x}| = \frac{1}{2}\boldsymbol{W}\boldsymbol{S}\boldsymbol{x} = \frac{1}{2}\boldsymbol{W}\boldsymbol{S}\boldsymbol{W}^H\boldsymbol{X} = \frac{1}{2}\boldsymbol{W}\boldsymbol{S}\boldsymbol{W}^H\boldsymbol{P}_0\boldsymbol{U}, \tag{26}$$

where $\boldsymbol{W}$ is the FFT matrix and $\boldsymbol{S}$ is a diagonal matrix whose entries on the main diagonal are the signs of $\boldsymbol{x}$. Then, Eq. (15) could be decomposed to

$$\boldsymbol{Y}_{odd} \triangleq \boldsymbol{P}_0{}^T\boldsymbol{Y} = \boldsymbol{P}_0{}^T\boldsymbol{X}_c + \boldsymbol{P}_0{}^T\boldsymbol{Z} = \frac{1}{2}\boldsymbol{U} + \boldsymbol{Z}_{odd}, \tag{27}$$

$$\boldsymbol{Y}_{even} \triangleq \boldsymbol{P}_e{}^T\boldsymbol{Y} = \boldsymbol{P}_e{}^T\boldsymbol{X}_c + \boldsymbol{P}_e{}^T\boldsymbol{Z} = \frac{1}{2}\boldsymbol{P}_e{}^T\boldsymbol{W}\boldsymbol{S}\boldsymbol{W}^H\boldsymbol{P}_0\boldsymbol{U} + \boldsymbol{Z}_{even}. \tag{28}$$

Collecting Eqs. (27) and (28) together, we have

$$\boldsymbol{R} = \boldsymbol{Q}\boldsymbol{U} + \boldsymbol{V}, \tag{29}$$

where

$$\boldsymbol{R} = \begin{bmatrix} \boldsymbol{Y}_{odd} \\ \boldsymbol{Y}_{even} \end{bmatrix}, \boldsymbol{Q} = \frac{1}{2}\begin{bmatrix} \boldsymbol{I} \\ \boldsymbol{P}_e{}^T\boldsymbol{W}\boldsymbol{S}\boldsymbol{W}^H\boldsymbol{P}_0\boldsymbol{U} \end{bmatrix}, \boldsymbol{V} = \begin{bmatrix} \boldsymbol{Z}_{odd} \\ \boldsymbol{Z}_{even} \end{bmatrix}, \tag{30}$$

where $\boldsymbol{I}$ denotes the identity matrix of proper size. Eq. (29) is a complete signal model of the received signal with respect to the information symbol. Therefore, based on Eq. (29), we can readily get the estimation of $\mathbf{U}$ by

$$\widehat{\boldsymbol{U}} = \begin{cases} (\boldsymbol{Q}^H\boldsymbol{Q})^{-1}\boldsymbol{Q}^H\boldsymbol{R}, & \boldsymbol{ZF} \\ (\boldsymbol{Q}^H\boldsymbol{Q}+\sigma_n{}^2\boldsymbol{I})^{-1}\boldsymbol{Q}^H\boldsymbol{R}, & \boldsymbol{MMSE} \end{cases} \tag{31}$$

Note that $\boldsymbol{Q}$ is in fact a function of $\mathbf{U}$ due to the component $\boldsymbol{S}$. However, at each iteration, we assume $\boldsymbol{Q}$ is known by substituting $\widehat{\boldsymbol{U}}$ from previous iteration to get $\boldsymbol{Q}$. At the first iteration, the basic receiver is used to get the initial estimate of $\widehat{\boldsymbol{U}}$.

5. Performance comparison

5.1. Spectral efficiency

In this section, we give a comparison on the spectral efficiencies of different optical OFDM systems.

For DCO-OFDM, each OFDM symbol only contains $N/2$ information-bearing complex-modulated symbols. Assuming the modulation order is M, then the spectral efficiency of DCO-OFDM is given by

$$\eta_{DCO-OFDM} = \frac{1}{2}\log_2 M \text{ bits/s/Hz}. \tag{32}$$

For all the non-DC-biased optical OFDM systems, as redundancy (zeros) is used in either frequency domain (ACO-OFDM and PAM-DMT) or time expansion is used (flip-OFDM), the spectral efficiencies are only half of DCO-OFDM:

$$\eta_{ACO-OFDM} = \eta_{PAM-DMT} = \eta_{Flip-OFDM} = \frac{1}{4}\log_2 M \text{ bits/s/Hz}. \tag{33}$$

For hybrid systems, things are a little bit complex. There is no general expression but one has to analyze the specific system.

For ADO-OFDM, in addition to a conventional ACO-OFDM transmission on odd subcarriers, a half-rate DCO-OFDM is used on even subcarriers. Therefore, its spectral efficiency is

$$\eta_{ADO-OFDM} = \eta_{ACO-OFDM} + \frac{1}{2}\eta_{DCO-OFDM} = \frac{1}{2}\log_2 M \text{ bits/s/Hz}. \tag{34}$$

For HACO-OFDM, a similar expression could be obtained:

$$\eta_{HACO-OFDM} = \eta_{ACO-OFDM} + \frac{1}{2}\eta_{PAM-DMT} = \frac{3}{8}\log_2 M \text{ bits/s/Hz}. \tag{35}$$

For eU-OFDM, the spectral efficiency depends on the number of layers. For an L-layer system, the spectral efficiency is given by

$$\eta_{eU-OFDM}(L) = \sum_{l=1}^{L}\left(\frac{1}{2}\right)^{l-1}\eta_{Flip-OFDM} = 2\left(1 - \frac{1}{2^{L-1}}\right)\eta_{Flip-OFDM}. \tag{36}$$

When L approaches infinity, we have the upper bound of spectral efficiency:

$$\eta_{eU-OFDM} = 2\eta_{Flip-OFDM} = \frac{1}{2}\log_2 M \text{ bits/s/Hz}. \tag{37}$$

There is a tradeoff between the spectral efficiency and decoding complexity with respect to *L:* a larger L means the spectral efficiency is closer to its upper bound but the decoding complexity, mainly from signal cancellation for decoded layers, will increase linearly with L. In practice, a fairly small L is desired to achieve a balance between the spectral efficiency and decoding complexity, say, for example, $L = 5$ is a good choice. In fact, when $L = 5$, we have

$$\eta_{eU-OFDM}(5) = 2\left(1 - \frac{1}{2^{5-1}}\right)\eta_{Flip-OFDM} = 0.94\eta_{eU-OFDM}, \tag{38}$$

which shows that the spectral efficiency is very close to the upper bound.

On summarizing, we can see that DCO-OFDM has the highest spectral efficiency. However, its power efficiency is not very good due to the non-information-bearing DC. On the contrary, the non-DC-biased optical OFDM systems have better power efficiency due to the elimination of DC offset but their spectral efficiency is only half of that of DCO-OFDM. The hybrid systems, especially ADO-OFDM and eU-OFDM, have better balance between the spectral efficiency and power efficiency. With those facts, one can choose a proper implementation form in practice under specific communication requirement and constraint.

5.2. Receiver complexity

The computational complexity of different receivers is analyzed here using the order notation. For the basic receiver, the main computation burden is the FFT and equalization, which have complexities of $O(N\log_2 N)$ and $O(N)$, respectively. In total, it is just $O(N\log_2 N)$. For the diversity combining receiver, it involves finite number of FFT/IFFT and a final equalization. Therefore, although it is more complex than the basic receiver, there is no difference when considering the order notation, that is, it is still $O(N\log_2 N)$. For the proposed iterative receiver, its main computation burden is the matrix inversion of Eq. (31) and this operation should be repeated at each iteration. Thus, the total complexity is in the order of $O(TN^3)$, where T is the total number of iterations. As we can see, this receiver is the most complicated one among the three receivers. However, as will be shown later, its performance is the best and can be far better than the other two. Thus, it is acceptable considering the performance gains. In addition, with the rapid development of modern signal-processing hardware, the computation burden will not be a limiting factor for these small-scale computations.

6. Simulations

In this section, we compare the average uncoded BER performance of different receivers in VLC channels through simulations. The channels are generated using the method in [15] with the following configurations: an empty room of size 8 × 6 × 4 m with reflection coefficients 0.8, 0.8, and 0.3 for the ceiling, the walls, and the floor, respectively; LEDs are used as the

http://dx.doi.org/10.5772/intechopen.68199

optical source and they are attached 0.1-m below the ceiling. The photodetectors (PDs) are 1 m above the floor with an 80° of field of view (FOV). Both line-of-sight (LOS) and nonline-of-sight (NLOS) channels are tested (the LEDs point straight downward and upward, respectively). Multiple LEDs and PDs are used to enhance the performance and robustness of the communication link, resulting in a multiple-input multiple-output (MIMO) channel model. The receiver design methods described in Section 4 can be easily extended to this channel model by using vector notation. For each MIMO channel realization, the positions of the LEDs and the photodetectors are randomly drawn from their corresponding plains and the channels are normalized to have power $N_R N_T$, where N_R and N_T denote the number of PDs and LEDs, respectively. The ill-conditioned channels are rejected for fair comparison. The number of subcarriers is N = 64. In the legend of figures, "conventional" denotes the basic receiver, "pairwise ML" denotes the receiver in [13], which is a special case of the diversity combining receiver. "Lower bound" denotes the ideal curve of the proposed receiver with perfect estimation of matrix $\boldsymbol{Q}$. In all receivers, MMSE equalization is used.

Figure 11 shows a sample view of the impulse response of the LOS and NLOS channels with a sampling rate of 300 MHz. It can be seen that the LOS channel is more like a delta function but NLOS channel has relatively longer delay spread, which means it can be viewed as a multipath channel.

First, we compare the BER performance in single-input single-output (SISO) channel. **Figure 12** shows the performance with modulation order M = 64. It can be seen that in LOS channel, the

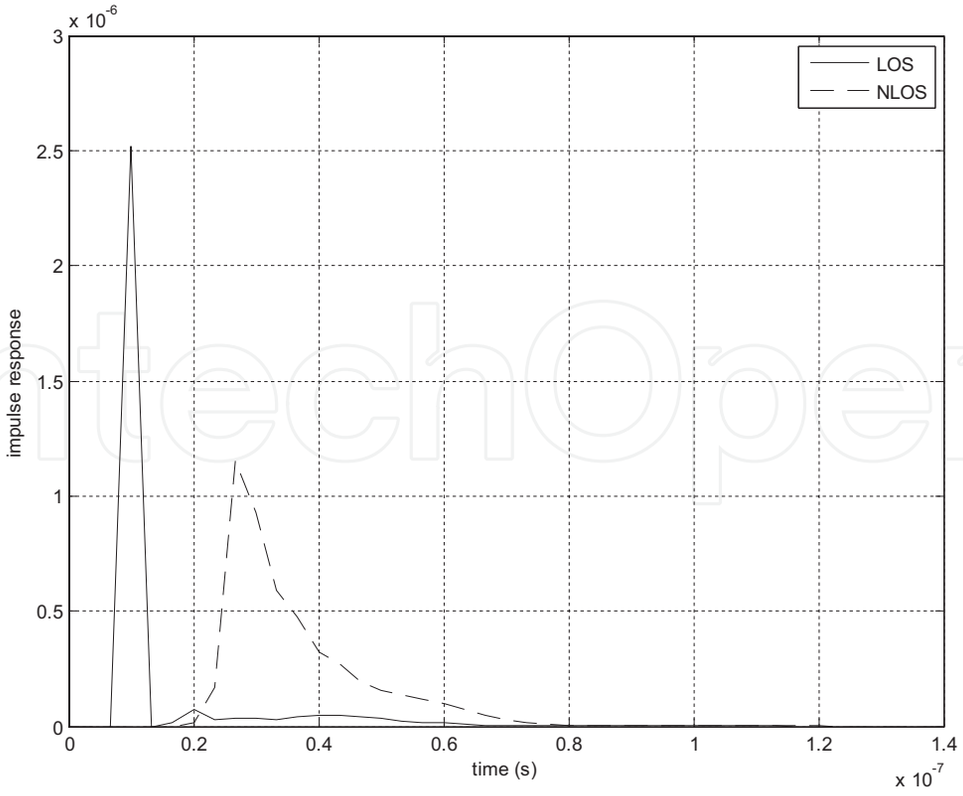


Figure 11. A sample view of LOS and NLOS channels with 300-MHz sampling rate.

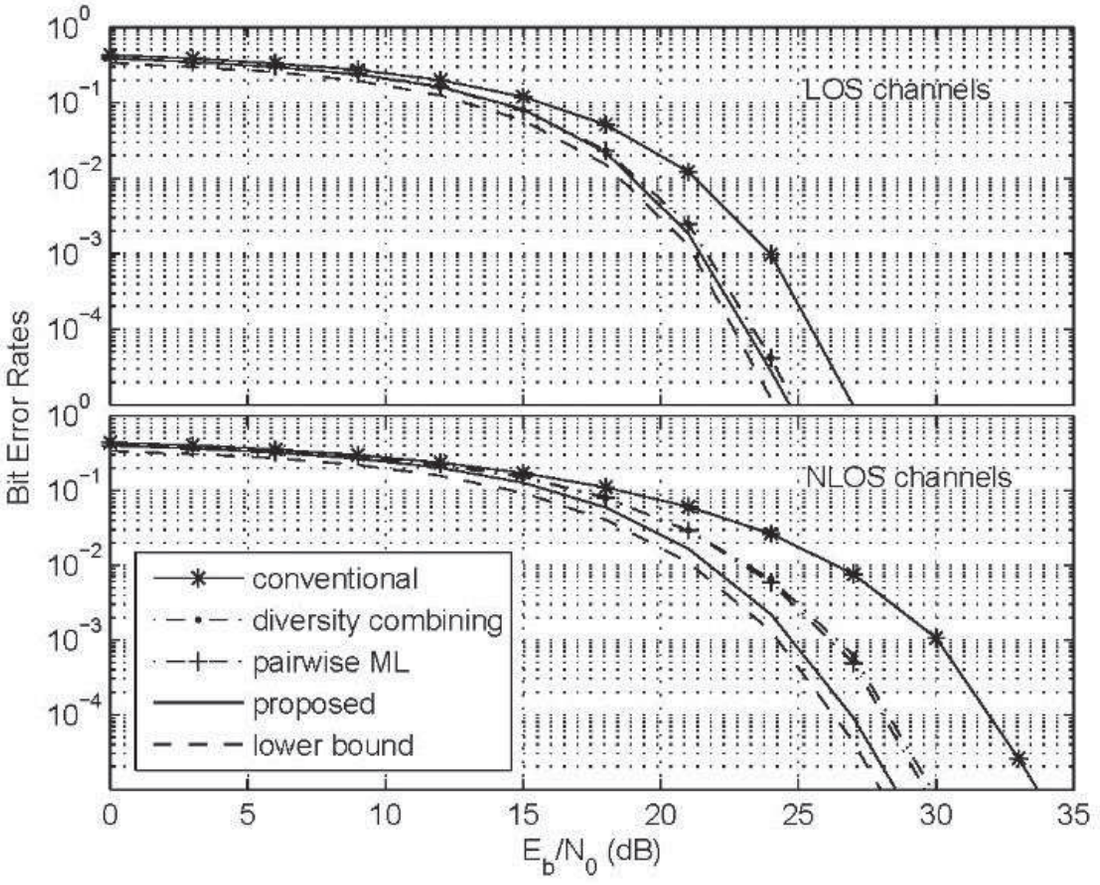


Figure 12. BER comparison of SISO ACO-OFDM using modulation sizes of $M = 64$.

diversity combining receiver and the proposed iterative receiver have similar performance and are much better than the basic receiver. In addition, their performance gap to the lower bound is limited. However, in NLOS channel, things are different: the proposed iterative receiver has the best performance. Compared to the basic receiver, its performance gain is more than 10 dB at high SNR range, which is significant. Even compared to the diversity combining receiver, 1-dB gain could be observed.

Now, we turn to MIMO channels. **Figure 13** shows the BER performance of a 4×4 MIMO ACO-OFDM using modulation sizes of $M = 16$. It can be seen that the performance of different receivers has similar behavior as the SISO case. However, compared to the SISO case, the performance gain of the proposed receiver is even larger: compared to the diversity combining receiver, it is more than 6 dB at high SNR regime; compared to the basic receiver, it is much more than 10 dB. Nonetheless, there is still a fairly large performance gap between the proposed receiver and its lower bound, which indicates that more advanced signal processing at the receiver side is desired in the future.

http://dx.doi.org/10.5772/intechopen.68199

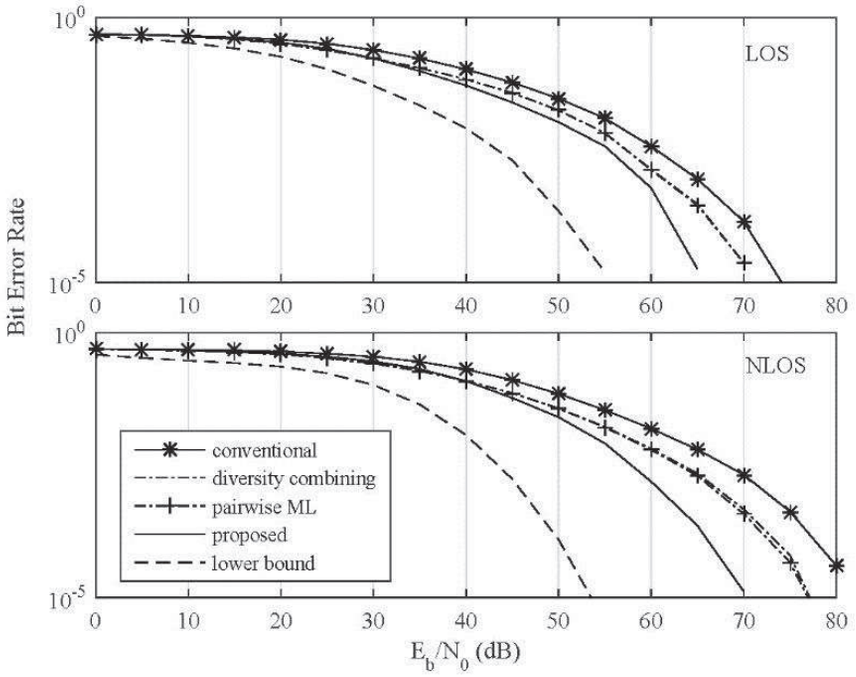


Figure 13. BER comparison of 4 × 4 MIMO ACO-OFDM using modulation sizes of $M = 16$.

7. Conclusions

In this research, we have investigated various forms of optical OFDM systems that are suitable for IM/DD optical channel. Different receivers are described with a proposed iterative one. Spectral efficiencies, computational complexities, as well as BER performance in LOS and NLOS channels of different systems and receivers are given. It is found that DCO-OFDM is more spectrally efficient than the non-DC-biased systems. The hybrid systems achieve a better tradeoff between the spectral efficiency and power efficiency. The proposed iterative receiver has the highest complexity but is far superior than other receivers, especially the basic receiver. Those results reveal the potential of OFDM systems in IM/DD channels for optical communication.

Acknowledgements

This work is supported by Southeast University 3-Category Academic Programs Project ("Optical Wireless Communication" and "Software-Defined Radio") and Top-notch Academic Programs Project of Jiangsu Higher Education Institutions (no. PPZY2015A035).

Author details

Jian Dang*, Liang Wu and Zaichen Zhang

*Address all correspondence to: newwanda@seu.edu.cn

School of Information Science and Engineering, Southeast University, Nanjing, P.R. China

References

[1] J. Armstrong, A. J. Lowery. Mint: Power efficient optical OFDM. Electronics Letters. 2006; **42**(6): 370–372. DOI: 10.1049/el:20063636.

[2] S. C. J. Lee, S. Randel, F. Breyer, A. M. J. Koonen. Mint: PAM-DMT for intensity-modulated and direct-detection optical communication systems. IEEE Photonics Technology Letters. 2009;**21**(23):1749–1751. DOI: 10.1109/LPT.2009.2032663.

[3] N. Fernando, Y. Hong, E. Viterbo. Mint: Flip-OFDM for unipolar communication systems. IEEE Transactions on Communications. 2012;**60**(12):3726–3733. DOI: 10.1109/TCOMM.2012.082712.110812.

[4] S. D. Dissanayake, K. Panta, J. Armstrong. A novel technique to simultaneously transmit ACO-OFDM and DCO-OFDM in IM/DD systems. In: IEEE GLOBECOM Workshops (GC Wkshps); 5–9 December 2011; Houston, Texas. IEEE; 2012. p. 782–786. DOI: 10.1109/GLOCOMW.2011.6162561.

[5] B. Ranjha, M. Kavehrad. Mint: Hybrid asymmetrically clipped OFDM-based IM/DD optical wireless system. Journal of Optical Communications and Networking. 2014;**6**(4):387–396. DOI: 10.1364/JOCN.6.000387.

[6] Q. Wang, Z. Wang, L. Dai. Mint: Asymmetrical hybrid optical OFDM for visible light communications with dimming control. IEEE Photonics Technology Letters. 2015;**27**(9):974–977. DOI: 10.1109/LPT.2015.2404972.

[7] D. Tsonev, S. Videv, H. Haas. Mint: Unlocking spectral efficiency in intensity modulation and direct detection systems. IEEE Journal on Selected Areas in Communications. 2015;**33**(9):1758–1770. DOI: 10.1109/JSAC.2015.2432530.

[8] J. Dang, Z. Zhang, L. Wu. Mint: Improving the power efficiency of enhanced unipolar OFDM for optical wireless communication. Electronics Letters. 2015;**51**(21):1681–1683. DOI: 10.1049/el.2015.2024.

[9] A. J. Lowery. Mint: Enhanced asymmetrically-clipped optical OFDM. Mathematics. 2015;**40**(1):36–40. DOI: 10.1364/OE.24.003950.

[10] M. S. Islim, D. Tsonev, H. Haas. On the superposition modulation for OFDM-based optical wireless communication. In: IEEE Global Conference on Signal and Information

Processing (Global SIP); 14–16 December 2015; Orlando, Florida, USA. IEEE; 2016. p. 1022–1026. DOI: 10.1109/GlobalSIP.2015.7418352.

[11] M. S. Islim, H. Haas. Mint: Augmenting the spectral efficiency of enhanced PAM-DMT-based optical wireless communications. Optics Express. 2016;**24**(11):11932–11949. DOI: 10.1364/OE.24.011932.

[12] L. Chen, B. Krongold, J. Evans. Diversity combining for asymmetrically clipped optical OFDM in IM/DD channels. In: IEEE Global Telecommunications Conference; 30 November–4 December 2009; Honolulu, Hawaii, USA. IEEE; 2010. p. 1–6. DOI: 10.1109/GLOCOM.2009.5425293.

[13] K. Asadzadeh, A. Dabbo, S. Hranilovic. Receiver design for asymmetrically clipped optical OFDM. In: IEEE GLOBECOM Workshops (GC Wkshps); 5–9 December 2011; Houston, Texas, USA. IEEE; 2012. p. 777–781. DOI: 10.1109/GLOCOMW.2011.6162559.

[14] J. Dang, Z. Zhang, L. Wu. Mint: A novel receiver for ACO-OFDM in visible light communication. IEEE Communications Letters. 2013;**17**(12):2320–2323. DOI: 10.1109/LCOMM.2013.111113.132223.

[15] J. B. Carruthers, P. Kannan. Mint: Iterative site-based modeling for wireless infrared channels. IEEE Transactions on Antennas Propagation. 2002;**50**(5):759–765. DOI: 10.1109/TAP.2002.1011244.

IntechOpen

IntechOpen

IntechOpen